GMR
The Original

GREEN-ENGINEERED MULTISCALE STARCH/PVA NANOFIBROUS SCAFFOLDS EMBEDDED WITH CUO NANOPARTICLES FROM *SARGASSUM ILICIFOLIUM* FOR POTENT ANTIMICROBIAL PERFORMANCE

Rajendra prasad Kunamalla[1], Mani Panagal[2], Chella Perumal Palanisamy[3]

[1]Department of Biotechnology, Annai College of Arts and Science (Affiliated to Bharathidasan University), Kovilacheri, Kumbakonam-612503, Tamil Nadu, India. Email: rp9907@gmail.com
[2]Department of Biotechnology, Annai College of Arts and Science (Affiliated to Bharathidasan University), Kovilacheri, Kumbakonam-612503, Tamil Nadu, India. Email: master.maniji@gmail.com, https://orcid.org/0000-0002-1597-1649
[3]Phytochemistry and Pharmacotherapy Lab, Department of Dermatology, Saveetha Medical College & Hospital (SMCH), Saveetha Institute of Medical and Technical Sciences (SIMATS), Thandalam, Chennai, Tamil Nadu 602105, India. Email: chellaperumalp.smc@saveetha.com, https://orcid.org/0000-0002-3527-3477

ABSTRACT
This study presents the development of a sustainable antimicrobial nanofibrous system by incorporating biosynthesized CuO NPs (copper oxide nanoparticles) into electrospun polymeric matrices. Aqueous extracts of the brown marine alga *Sargassum ilicifolium* were utilized for ultrasonic-assisted extraction, enabling an environmentally friendly nanoparticle synthesis process. The resulting CuO NPs exhibited nanoscale dimensions (~108 nm), monoclinic crystallinity, and moderate dispersion stability (−18.3 mV), as confirmed through UV–Vis, FTIR, XRD, SEM, TGA, and DLS analyses. These nanoparticles were homogeneously embedded within starch/PVA solutions and electrospun to produce uniform, bead-free fibers with a porous architecture. Antimicrobial performance was evaluated against pathogenic microorganisms. The nanoscaffolds (50 µg/mL) demonstrated superior inhibitory activity compared to both the algal extract and standalone nanoparticles, with maximum zones observed for E. coli (31±0.16 mm) and Penicillium sp. (27±0.23 mm). The fabricated polymeric nanoscaffolds promoting effective microbial contact and sustained ion release, highlighting their potential as eco-friendly antimicrobial biomaterials.

KEYWORDS: *Sargassum ilicifolium*, biosynthesis, CuO nanostructures, Electrospun fibers, Starch-PVA composites, Antimicrobial performance.

1. INTRODUCTION
The increasing prevalence of microbial infections, coupled with the rapid emergence of antibiotic-resistant pathogens, represents a critical challenge to modern healthcare systems [1]. Conventional antimicrobial agents are becoming progressively less effective, particularly against multidrug-resistant bacteria and opportunistic fungi [2,3]. In this regard, nanotechnology has emerged as a transformative approach, offering innovative solutions through the development of nanostructured antimicrobial systems [4]. Metal oxide nanomaterials have been widely investigated for antimicrobial applications due to their strong biological activity and stable physicochemical nature [5]. Among them, copper oxide nanoparticles (CuO NPs) have attracted particular attention because of their effectiveness against a wide range of microorganisms, including both bacteria and fungi. Their antimicrobial action is attributed to several simultaneous processes, such as the generation of reactive oxygen species, disruption of microbial cell membranes, and the release of copper ions. Together, these mechanisms enhance microbial killing efficiency while also reducing the likelihood of resistance development [6].
Although these nanomaterials offer significant benefits, traditional nanoparticle fabrication techniques frequently rely on hazardous reagents and high-energy conditions, which pose risks to both environmental sustainability and human health. In response to these challenges, eco-friendly synthesis strategies based on biological systems have emerged as a viable alternative, gaining increasing attention in recent years [7]. Biological extracts obtained from terrestrial plants and marine sources are rich in diverse phytochemicals that can facilitate nanoparticle formation by functioning as both reducing and capping agents. Among these, marine macroalgae especially brown species such as *Sargassum ilicifolium* are particularly valuable due to their abundance of phenolics, polysaccharides, and various secondary metabolites, which make them excellent candidates for sustainable nanoparticle synthesis [8]. Additionally, these marine-derived compounds may further enhance the biological activity of the synthesized nanoparticles [9].
Parallel to nanoparticle development, the design of functional biomaterials capable of delivering antimicrobial agents in a controlled and efficient manner has become increasingly important [10]. Electrospinning-based nanofibrous scaffolds have attracted considerable interest owing to their resemblance to the native extracellular matrix, along with their large surface-to-volume ratio, adjustable pore structure, and capacity for controlled delivery of therapeutic agents. Among the

materials used, natural polymers such as starch are especially appealing for scaffold development due to their inherent biodegradability, excellent biocompatibility, and wide availability. However, their inherent limitations, including poor mechanical strength and high hydrophilicity, can be effectively overcome by blending with synthetic polymers such as polyvinyl alcohol (PVA), resulting in improved mechanical stability and processability [11].

Integrating biogenically synthesized nanoparticles into electrospun polymeric matrices offers a promising strategy for developing multifunctional antimicrobial systems [12]. Such hybrid materials can combine the potent antimicrobial activity of nanoparticles with the structural advantages of nanofibrous scaffolds, leading to enhanced surface interactions with microbial cells and controlled release of active components [13]. This synergistic approach has significant potential in biomedical applications, including wound dressings, tissue engineering, and protective coatings.

In this context, the present study aims to develop eco-friendly electrospun nanoscaffolds composed of starch/PVA incorporated with *Sargassum ilicifolium*-mediated CuO nanoparticles, and to evaluate their physicochemical characteristics and antimicrobial efficacy against clinically relevant bacterial and fungal pathogens.

2. Experimental Section

2.1. Collection and preparation of marine macroalgae

Fresh samples of the brown marine macroalga *Sargassum ilicifolium* were collected from the intertidal coastal region of Rameswaram, India. To preserve their bioactive components, the collected material was promptly transported to the laboratory under cooled conditions. The samples were then thoroughly cleaned to remove sand, debris, and associated organisms. The dried material was subsequently converted into a fine powder and stored in airtight containers at ambient conditions for further use in extraction.

2.2. Ultrasound-enhanced extraction of secondary metabolites

To obtain bioactive compounds from the algal material, an ultrasound-assisted extraction approach was adopted to enhance extraction efficiency. Briefly, 2 g of dried algal powder was mixed with 50 mL of purified water to form a uniform suspension. The mixture was then subjected to sonication at 60 °C for 45 minutes. The ultrasonic treatment facilitated the breakdown of cell structures, allowing the release of intracellular compounds such as phenolics, flavonoids, and polysaccharides into the solvent. After extraction, the mixture was allowed to cool and then filtered to remove solid residues, resulting in a clear extract. The filtrate was stored at low temperature for short-term use and later converted into a dry powder through freeze-drying. This stable extract was preserved under suitable conditions [14].

2.3. Green synthesis of CuO NPs

Copper oxide nanoparticles were synthesized through an eco-friendly approach using algal-derived biomolecules as reducing agents, thereby avoiding the use of harmful chemicals. In brief, an aqueous copper salt solution was prepared and mixed with *Sargassum ilicifolium* extract in an appropriate ratio to initiate the reaction. The mixture was maintained under controlled temperature and continuous stirring to facilitate the reduction of copper ions. During the process, a noticeable color change from blue to greenish-blue was observed, indicating the formation of copper oxide nanoparticles. This transformation is attributed to the interaction between copper ions and bioactive compounds present in the algal extract, which also help stabilize the formed nanoparticles. After completion of the reaction, the nanoparticles were separated, purified through repeated washing to remove impurities, and then dried to obtain a stable powder. The final product was stored under suitable conditions and later used for further analysis and fabrication of nanofibrous scaffolds [15].

2.4. Electrospinning of CuO-embedded starch/PVA nanofibrous scaffolds

Nanofibrous scaffolds incorporating copper oxide nanoparticles were prepared using an electrospinning approach to obtain a porous and uniform fibrous structure. A solution of polyvinyl alcohol was first prepared in water until a clear and homogeneous mixture was formed. Starch and the synthesized CuO nanoparticles were then added and mixed thoroughly to ensure uniform distribution within the polymer matrix. The resulting solution was processed to generate continuous nanofibers under optimized conditions, leading to the formation of smooth and defect-free fibrous mats. The process was carried out under ambient conditions for several hours to allow sufficient fiber deposition. After fabrication, the nanofibrous mats were carefully collected and stored in a dry environment to prevent moisture absorption and to preserve their structural integrity for subsequent analyses [16-18].

2.5. Physicochemical characterization

The optical characteristics of the algal extract and the synthesized copper oxide nanoparticles were analyzed by recording absorption spectra within the range of 200–800 nm. Deionized water was used as a reference during measurements. The appearance of distinct absorption features in the nanoparticle sample confirmed the successful formation of copper oxide, while also indicating interactions between metal ions and bioactive constituents present in the extract [19].

The chemical composition and functional groups associated with both the nanoparticles and the composite scaffolds were examined using infrared spectroscopy. Spectral data collected over a broad wavenumber range enabled the identification of key functional groups, including hydroxyl, carbonyl, phenolic, and metal–oxygen bonds. These observations confirmed the formation of nanoparticles and their interaction with the polymeric matrix [20].

Crystallographic properties of the synthesized nanoparticles and the composite scaffolds were assessed through diffraction analysis. The recorded diffraction patterns were compared with standard reference data to confirm the crystalline phase and structural purity of the materials [21].

The surface morphology and structural organization of the nanoparticles and electrospun fibers were evaluated through microscopic imaging. The images provided information on particle shape, fiber uniformity, surface characteristics, and the distribution of nanoparticles within the scaffold framework [22].
Thermal behavior of the fabricated scaffolds was investigated by monitoring weight changes under controlled heating conditions. The resulting thermal profiles revealed information regarding moisture loss, decomposition stages, and overall stability of the material [23].
Particle size distribution and dispersion stability of the nanoparticles were analyzed using light scattering techniques. Measurements of hydrodynamic diameter and surface charge provided insight into particle size variability and colloidal stability, where higher surface charge values indicated improved resistance to aggregation in suspension [24]. All experimental datasets generated during this study are publicly accessible via the Mendeley Data repository (DOI: 10.17632/vf8822rd8j.1.)

2.6. Evaluation of antimicrobial activity

The antimicrobial potential of the algal extract, biosynthesized copper oxide nanoparticles, and CuO-incorporated starch/PVA nanofibrous scaffolds was evaluated against selected pathogenic microorganisms using a standard diffusion method. All samples were examined at a concentration of 50 µg/mL. The test panel included Gram-negative bacteria (Escherichia coli, Klebsiella pneumoniae, and Citrobacter koseri), a Gram-positive bacterium (Staphylococcus aureus), and fungal strains (Aspergillus niger and Penicillium sp.), representing commonly encountered pathogens. For bacterial evaluation, cultures were adjusted to a standardized cell density equivalent to 0.5 McFarland and evenly spread across nutrient agar surfaces. Fungal strains were cultured on appropriate agar media under similar conditions. Wells of uniform size were created in the agar, and equal volumes of each sample were introduced into the designated wells. Standard antimicrobial agents were included as reference controls for comparison in both bacterial and fungal studies. After allowing sufficient time for diffusion of the test materials into the agar, the plates were incubated under suitable temperature conditions specific to each microorganism. Following incubation, antimicrobial activity was determined by measuring the clear zones surrounding each well, expressed in millimeters. All experiments were repeated three times under consistent conditions to ensure accuracy and reproducibility of the results [25,26].

2.7. Statistical analysis

The obtained data were analyzed statistically and are expressed as mean ± standard deviation based on three independent trials. Differences between groups were assessed using appropriate variance analysis, followed by post hoc comparisons when necessary. A value of $p < 0.05$ was considered to indicate statistical significance [27].

3. RESULTS

3.1. UV–visible spectroscopy

The optical properties of the *Sargassum ilicifolium* extract and the synthesized copper oxide nanoparticles were analyzed by recording their absorption spectra across a broad wavelength range (Fig. 1). The algal extract showed distinct absorption patterns, which can be linked to the presence of naturally occurring bioactive compounds. In comparison, the nanoparticle sample exhibited characteristic absorption features that indicate the successful formation of copper oxide at the nanoscale. Clear differences between the extract and nanoparticle spectra confirm the conversion of copper ions into nanoparticles. While the extract maintained its typical phytochemical absorption profile, the nanoparticles displayed new optical characteristics associated with their formation, highlighting the role of algal constituents in the synthesis process.

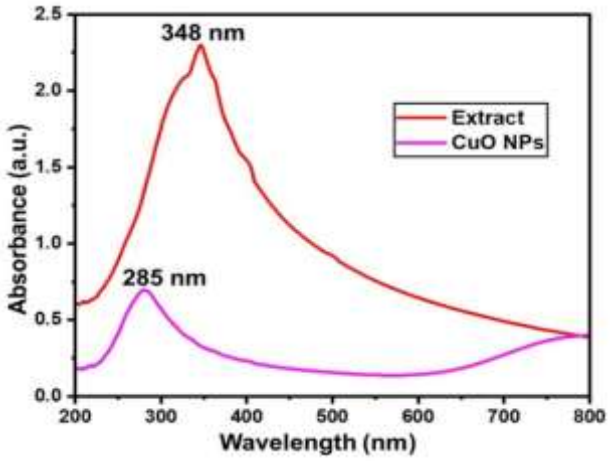

Fig. 1. UV–visible absorption spectra illustrating the optical characteristics of *Sargassum ilicifolium* extract and the synthesized copper oxide nanoparticles.

3.2. FTIR spectroscopy analysis

The chemical composition of the synthesized copper oxide nanoparticles and the CuO-loaded starch/PVA nanofibrous scaffolds was examined through infrared spectral analysis (Fig. 2). The nanoparticles displayed several distinct absorption bands, which are associated with metal–oxygen bonding along with surface functional groups derived from the biological

synthesis process. These features confirm the successful formation of copper oxide at the nanoscale. For the electrospun starch/PVA scaffolds, characteristic absorption peaks corresponding to hydroxyl, carbonyl, ether, and hydrocarbon groups were observed, indicating the presence of both polymeric and polysaccharide components within the fibrous matrix. In addition, minor shifts and broadening of specific absorption bands were noted in the composite scaffolds, suggesting interactions between the nanoparticles and functional groups present in the polymer network. These changes provide clear evidence for the effective incorporation and stabilization of CuO nanoparticles within the electrospun structure.

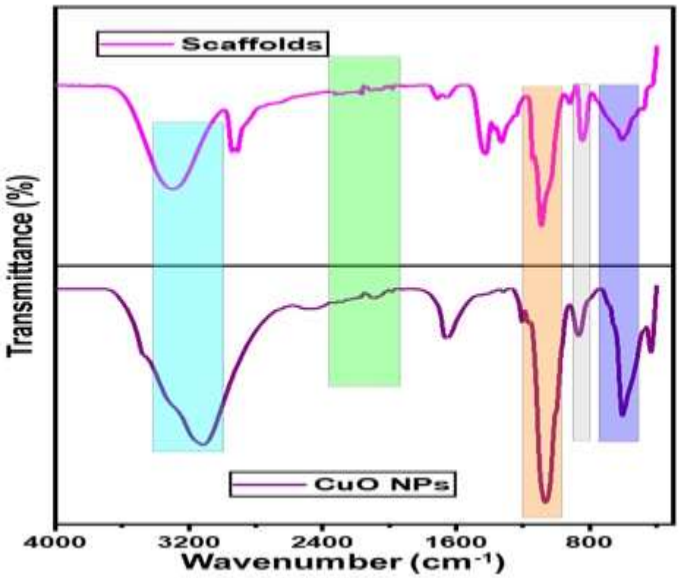

Fig. 2. FTIR spectral analysis of biosynthesized CuO nanoparticles and CuO-integrated starch/PVA electrospun nanoscaffolds, highlighting functional group interactions and nanoparticle incorporation.

3.3. XRD analysis

The crystalline nature of the synthesized copper oxide nanoparticles and the CuO-loaded starch/PVA nanofibrous scaffolds was evaluated using diffraction analysis (Fig. 3). The nanoparticles showed sharp and well-defined diffraction peaks, indicating a highly ordered crystalline structure consistent with copper oxide. The narrow peak profiles suggest good crystallinity, and the calculated crystallite size confirmed that the particles were within the nanoscale range. In contrast, the diffraction pattern of the polymer-based scaffolds displayed broader peaks, reflecting their semi-crystalline nature. This reduction in crystallinity is attributed to the incorporation of nanoparticles into the polymer matrix, which disrupts the regular arrangement of polymer chains. Importantly, no additional peaks related to impurities were detected, confirming the purity of the synthesized nanoparticles and their successful integration into the scaffold system without the formation of unwanted secondary phases.

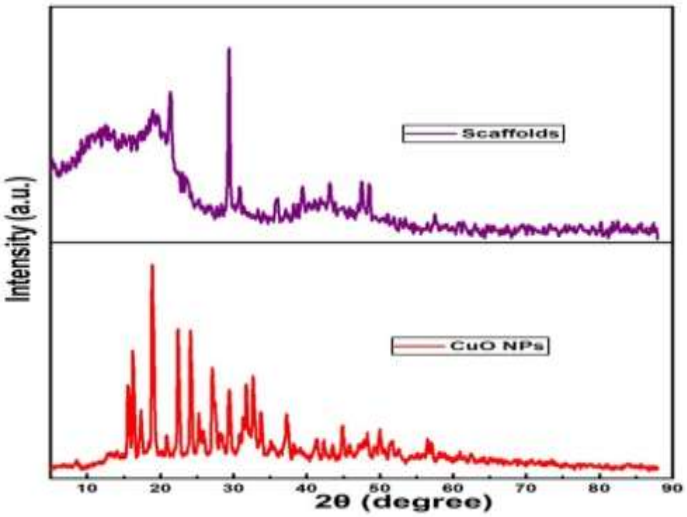

Fig. 3. X-ray diffraction profiles of biosynthesized CuO nanoparticles and CuO-incorporated starch/PVA nanofibrous scaffolds, demonstrating crystalline characteristics and successful nanoparticle integration.

3.4. SEM analysis

The surface morphology of the synthesized copper oxide nanoparticles and the electrospun starch/PVA nanofibrous scaffolds was analyzed using microscopic imaging (Fig. 4). The nanoparticles appeared as well-defined particles with a combination of shapes, mainly spherical along with some irregular forms. Their slightly rough surface texture suggests a

crystalline nature. In comparison, the electrospun scaffolds exhibited a highly porous and interconnected fibrous network. The fibers were evenly distributed, showed uniform thickness, and were largely free of bead formation, indicating efficient processing and uniform mixing of the components. The smooth appearance of the fibers further reflects proper integration of the nanoparticles within the polymer matrix. Overall, these observations confirm the successful formation of continuous nanofibrous structures with high porosity and surface area, which are beneficial for applications such as drug delivery, tissue regeneration, and other biomedical uses.

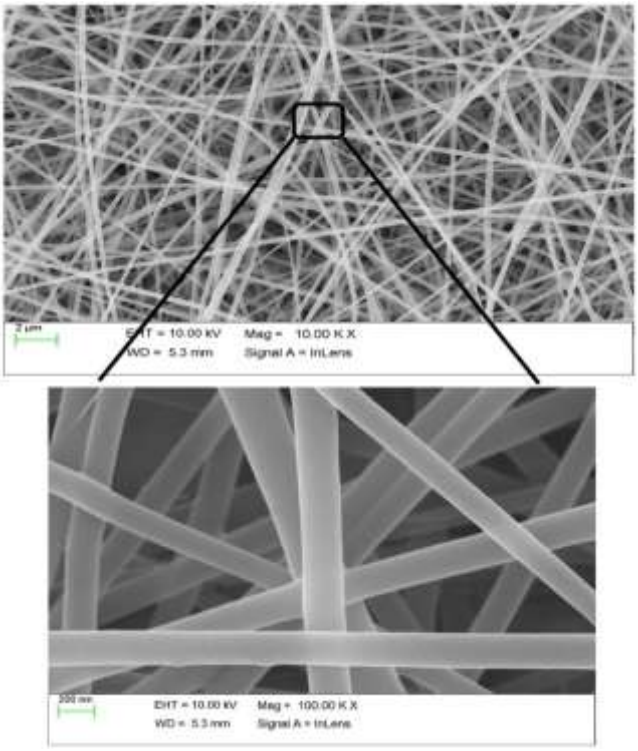

Fig. 4. Scanning electron microscopy images depicting the morphology of biosynthesized CuO nanoparticles and CuO-integrated starch/PVA electrospun nanoscaffolds, highlighting particle shape and fibrous architecture.

3.5. TGA

The thermal behavior of the starch/PVA nanofibrous scaffolds was evaluated by monitoring changes in weight as the temperature increased (Fig. 5). The material began to show signs of degradation at around 232°C, marking the initial stage of weight loss. A major decomposition phase occurred near 327°C, indicating significant breakdown of the polymer structure. The degradation process was largely completed by approximately 374°C, resulting in an overall weight loss of about 38%. At lower temperatures, a gradual reduction in mass was observed, which can be attributed to the evaporation of moisture and other volatile components. This was followed by a more rapid decrease in weight at higher temperatures, corresponding to the decomposition of the organic polymer network. These results indicate that the developed nanoscaffolds exhibit moderate thermal stability with a clear degradation pattern, suggesting their suitability for biomedical applications where controlled thermal behavior is required.

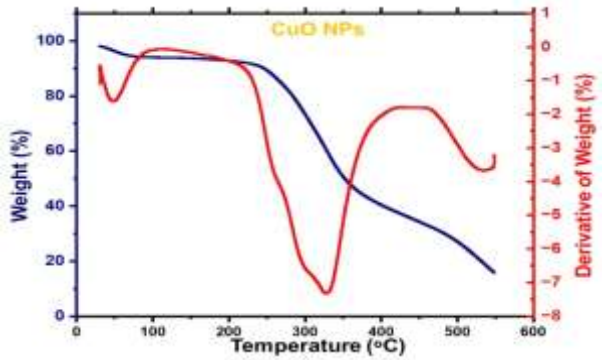

Fig. 5. Thermogravimetric analysis illustrating the thermal stability and decomposition profile of CuO-loaded starch/PVA electrospun nanoscaffolds.

3.6. Zeta potential and particle size analysis

The particle size distribution and dispersion behavior of the synthesized copper oxide nanoparticles were analyzed using light scattering techniques (Fig. 6). The results showed an average particle size of approximately 108 nm. A relatively

high polydispersity index (0.7317) indicates that the particles are not uniform in size and exhibit moderate variability. The surface charge of the nanoparticles was also examined to understand their stability in suspension (Fig. 7). The particles exhibited a negative charge with an average value of –18.3 mV, along with additional distributions at more negative and less negative values. This indicates the presence of electrostatic repulsion between particles, which helps in maintaining dispersion and reducing aggregation. Overall, the nanoparticles demonstrated moderate stability in solution along with a broad size range, which could influence their effectiveness in applications such as drug delivery, sensing systems, and catalytic processes.

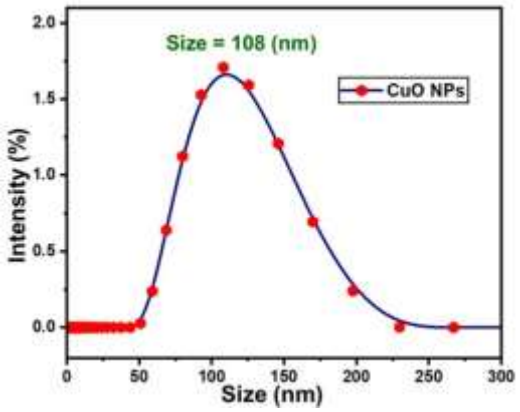

Fig.6. Dynamic light scattering profile showing the hydrodynamic particle size distribution of biosynthesized CuO nanoparticles.

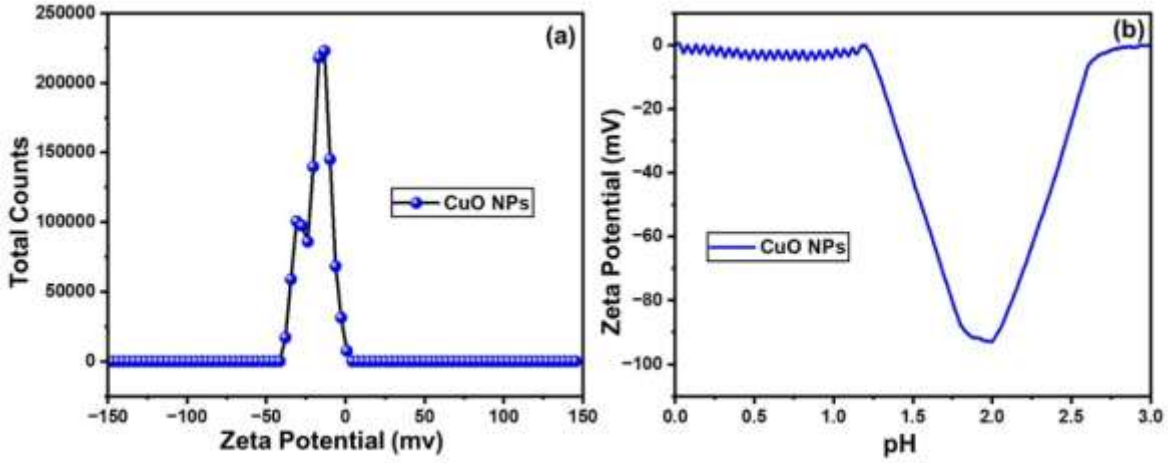

Fig.7. Zeta potential profile of biosynthesized CuO nanoparticles, indicating surface charge characteristics and colloidal stability.

3.7. Antimicrobial efficacy

The antimicrobial assessment revealed distinct differences in inhibitory performance among the tested samples (Table 1). For bacterial pathogens, the Sargassum ilicifolium extract exhibited moderate antibacterial activity, producing inhibition zones of 22±0.28 mm against Escherichia coli, 22±0.23 mm against Klebsiella pneumoniae, 23±0.19 mm against Staphylococcus aureus, and 24±0.24 mm against Citrobacter koseri. The CuO nanoparticles demonstrated comparatively improved activity, with inhibition zones ranging from 25±0.15 mm for S. aureus to 29±0.12 mm for E. coli. Notably, the CuO-loaded nanofibrous scaffolds showed the highest antibacterial efficacy, particularly against E. coli (31±0.16 mm) and K. pneumoniae (28±0.26 mm), indicating enhanced performance due to nanoparticle incorporation within the polymer matrix.

Table 1: Comparative evaluation of antimicrobial activity exhibited by *Sargassum ilicifolium* extract, biosynthesized CuO nanoparticles, and CuO-incorporated starch/PVA electrospun nanofibrous scaffolds (50 µg/mL) against selected bacterial and fungal pathogens.

Organisms	Zone of inhibition (mm)				
	Ciprofloxacin (Antibiotic)	Voriconazole (Antifungal)	Algal Extract	CuO NPs	Nano-scaffolds
Escherichia coli	33±0.58	-	22±0.28	29±0.12	31±0.16
Klebsiella pneumoniae	30±0.14	-	22±0.23	26±0.32	28±0.26

Staphylococcus aureus	28±0.32	-	23±0.19	25±0.15	26±0.14
Citrobacter koseri	29±0.47	-	24±0.24	25±0.28	28±0.25
Aspergillus niger	-	26±0.65	21±0.28	23±0.24	25±0.16
Penicillium species	-	28±0.39	23±0.13	25±0.32	27±0.23

A similar trend was observed for antifungal activity. The algal extract produced inhibition zones of 21±0.28 mm against Aspergillus niger and 23±0.13 mm against Penicillium sp., whereas CuO nanoparticles exhibited slightly improved inhibition of 23±0.24 mm and 25±0.32 mm, respectively. In contrast, the nanoscaffolds demonstrated superior antifungal effects, with inhibition zones of 25±0.16 mm for A. niger and 27±0.23 mm for Penicillium sp.
When compared with standard antimicrobial agents, ciprofloxacin (for bacteria) and voriconazole (for fungi) produced higher inhibition zones, such as 33±0.58 mm against E. coli and 28±0.39 mm against Penicillium sp., thereby validating the experimental methodology. Overall, the results clearly indicate that the nanoscaffold system exhibits enhanced and broad-spectrum antimicrobial activity relative to the individual components, highlighting its potential as an effective antimicrobial platform.

4. DISCUSSION

A comprehensive evaluation of the physicochemical and biological characteristics of *Sargassum ilicifolium*-mediated CuO nanoparticles and their incorporation into starch/PVA electrospun scaffolds provides significant insights into their functional performance as antimicrobial biomaterials. The collective outcomes obtained from spectroscopic, structural, morphological, thermal, and biological analyses demonstrate a clear relationship between material composition, nanoscale architecture, and enhanced bioactivity.
The UV–Visible spectral analysis confirmed the successful formation of CuO nanoparticles, as evidenced by the appearance of characteristic absorption bands associated with metal oxide nanostructures. These optical features arise from electronic transitions influenced by the nanoscale dimensions of the particles and reflect the effective reduction of copper ions mediated by phytochemicals present in the algal extract. In contrast, the extract exhibited broad absorption in the UV region, corresponding to naturally occurring compounds such as phenolics and flavonoids, which are known to play a dual role as reducing and stabilizing agents during nanoparticle synthesis. The distinct spectral shift between the extract and nanoparticle system clearly indicates the transformation process and validates the green synthesis strategy [28].
Further insight into the chemical interactions within the system was provided by FTIR analysis. The presence of characteristic Cu–O vibrational bands confirmed the formation of copper oxide, while the detection of functional groups such as hydroxyl, carbonyl, and ether linkages in the polymeric scaffolds highlighted the structural integrity of the starch/PVA matrix. Notably, subtle shifts and peak broadening observed after nanoparticle incorporation suggest intermolecular interactions between CuO nanoparticles and the polymer chains. Such interactions are critical for ensuring uniform nanoparticle dispersion, which in turn contributes to improved mechanical stability and functional performance of the composite scaffolds [29-31].
XRD analysis supported these findings by revealing well-defined diffraction peaks corresponding to the monoclinic phase of CuO, confirming the crystalline nature of the synthesized nanoparticles. The relatively sharp peaks indicated high crystallinity at the nanoscale, while the broader peaks observed in the scaffold matrix reflected its semi-crystalline polymeric structure. Importantly, the absence of additional peaks in the composite system indicates that the incorporation of nanoparticles did not introduce any secondary phases, thereby preserving the structural integrity of both components [32,33].
Morphological observations obtained through SEM further reinforced the successful fabrication of the nanocomposite system. The CuO nanoparticles exhibited defined shapes with rough surfaces, indicative of crystalline features, whereas the electrospun scaffolds displayed a highly porous and interconnected fibrous network with uniform, bead-free morphology. This structural organization is particularly advantageous for biomedical applications, as it enhances surface area, facilitates cell interaction, and allows efficient diffusion of nutrients and bioactive agents. The homogeneous distribution of nanoparticles within the fibers also suggests effective blending and optimized electrospinning conditions [34,35].
Thermal analysis demonstrated that the fabricated scaffolds possess moderate thermal stability, with degradation occurring in well-defined stages corresponding to moisture loss and polymer decomposition. The observed thermal behavior is consistent with biodegradable polymer systems and indicates that the scaffolds can retain their structural integrity under physiological conditions. This property is essential for applications where thermal resistance and material durability are required [34,36].
The DLS and zeta potential measurements revealed that the CuO nanoparticles possess nanoscale dimensions and moderate colloidal stability. The negative surface charge observed suggests sufficient electrostatic repulsion to minimize particle aggregation in suspension, thereby maintaining dispersion stability. Although a certain degree of size variability was observed, the overall characteristics remain suitable for biomedical applications, where nanoscale dimensions play a critical role in enhancing biological interactions [37-39].
Most notably, the antimicrobial studies clearly demonstrated the superior performance of the CuO-loaded nanoscaffolds compared to both the algal extract and standalone nanoparticles. While the extract exhibited moderate antimicrobial effects

due to its bioactive constituents, the CuO nanoparticles showed enhanced activity, particularly against Gram-negative bacteria, likely due to their thinner cell wall structure and increased susceptibility to nanoparticle-induced damage. The nanoscaffolds, however, exhibited the highest level of antimicrobial efficacy across all tested strains. This enhanced performance can be attributed to the synergistic interaction between the nanoparticles and the nanofibrous matrix, which enables sustained release of copper ions and increased contact with microbial cells. The porous architecture of the scaffolds further amplifies this effect by facilitating greater surface interaction and localized antimicrobial action [27,40]. In comparison with standard antimicrobial agents, the nanoscaffolds demonstrated comparable levels of inhibition, underscoring their potential as alternative antimicrobial materials. The integration of biologically synthesized nanoparticles into a biodegradable polymer matrix not only enhances antimicrobial efficiency but also provides a platform for controlled delivery and improved material functionality.

Overall, this study highlights the effectiveness of combining green synthesis approaches with advanced nanofabrication techniques to develop multifunctional biomaterials. The resulting nanoscaffolds exhibit a unique combination of structural integrity, thermal stability, and potent antimicrobial activity, making them promising candidates for applications such as wound healing, tissue engineering, and biomedical coatings. Furthermore, the use of marine-derived resources such as *Sargassum ilicifolium* aligns with sustainable material development and opens new avenues for the utilization of natural bioresources in nanotechnology-driven healthcare solutions.

5. CONCLUSION

This study presents an environmentally sustainable strategy for the synthesis of copper oxide nanoparticles utilizing *Sargassum ilicifolium* extract, followed by their successful integration into starch/PVA-based electrospun nanofibrous scaffolds. Detailed physicochemical analyses confirmed the formation of crystalline nanoparticles, their stable incorporation within the polymeric matrix, and the overall structural and thermal robustness of the developed system. The resulting scaffolds exhibited a well-defined porous architecture with uniform fiber morphology, which is advantageous for biomedical functionality. Biological evaluation demonstrated that the CuO-incorporated nanoscaffolds possess significantly enhanced antimicrobial activity against both bacterial and fungal pathogens when compared to the extract and nanoparticles alone, indicating a clear synergistic effect. This improved performance is likely attributed to the combined influence of nanoparticle activity and the high surface area of the fibrous network, enabling effective microbial interaction and sustained release of active species. Overall, the findings emphasize the potential of marine-derived, green-synthesized nanocomposites as efficient antimicrobial platforms. The developed system offers a promising, biocompatible, and sustainable alternative for applications in wound management, drug delivery, and tissue engineering, and warrants further investigation for clinical translation.

Data Availability Statement: The full dataset of physiochemical characterization associated with this work is published in Mendeley Data [Dataset] Innovative green composites: Material characterization of starch-based nanoscaffolds reinforced with Sargassum ilicifolium-mediated copper oxide nanostructures (DOI: 10.17632/4kdtskdtmc.2)**. Disclosure:** The material characterization data and figures (e.g., UV, SEM, FTIR, XRD, TGA, Zeta Potential and particle sizer) presented here were generated from a common dataset and are being reused across multiple related studies on nanomaterials. All biological analyses and conclusions are original to each manuscript.

Conflicts of Interest: The authors declare no conflicts of interest.

REFERENCES

1. Kumaravelu, P.; Shanmugam, R.; Jayakodi, S. Advances in Nanoparticle-Based Mechanisms and Therapeutic Applications for Lung Cancer. BioNanoScience 2025, 15(3), 522.
2. Kumaravelu, P.; Shanmugam, R.; Jayakodi, S. Advancements in medicinal plant-derived trace element nanoparticles for diabetes mellitus therapy. BioNanoScience, 2025, 15(3), 429.
3. Savio, S.; Varghese, R.M.; Subramanian, A.K.; Shanmugam, R. Nanoparticle-based oral rinse in prevention of white spot lesions in orthodontic treatment: A systematic review. Journal of Orthodontic Science 2025; 14(1), 33.
4. Saleem, M. H.; Ejaz, U.; Vithanage, M.; Bolan, N.; Siddique, K. H. Clean Technologies and Environmental Policy 2024, 1-26.
5. Guan, G.; Zhang, L.; Zhu, J.; Wu, H.; Li, W.; Sun, Q. Journal of Hazardous Materials 2021, 402, 123542.
6. Khan, F.; Shahid, A.; Zhu, H.; Wang, N.; Javed, M. R.; Ahmad, N.; Xu, J.; Alam, M. A.; Mehmood, M. A. Chemosphere 2022, 293, 133571.
7. Ahmed, S. F.; Mofijur, M.; Rafa, N.; Chowdhury, A. T.; Chowdhury, S.; Nahrin, M.; Islam, A. S.; Ong, H. C. Environmental Research 2022, 204, 111967.
8. Durga, M.; Deepikaa, R.; Vaishnavi, M.; Raksha, B. Saudi J Med Pharm Sci 2024, 10, 489-501.
9. Menaa, F.; Wijesinghe, U.; Thiripuranathar, G.; Althobaiti, N. A.; Albalawi, A. E.; Khan, B. A.; Menaa, B. Marine drugs 2021, 19, 484.
10. Rajabi, H. R.; Alvand, Z. M.; Mirzaei, A. Environmental Science and Pollution Research 2023, 30, 120236-120249.
11. Avcu, E.; Bastan, F. E.; Guney, M.; Avcu, Y. Y.; Rehman, M. A. U.; Boccaccini, A. R. Acta Biomaterialia 2022, 151, 1-44.
12. Kirillova, A.; Yeazel, T. R.; Asheghali, D.; Petersen, S. R.; Dort, S.; Gall, K.; Becker, M. L. Chemical reviews 2021, 121, 11238-11304.
13. Arruda, T. R.; Machado, G. d. O.; Marques, C. S.; Souza, A. L. d.; Pelissari, F. M.; Oliveira, T. V. d.; Silva, R. R. A. Macromol 2025, 5, 19.

14. Martín-del-Campo, A.; Fermín-Jiménez, J. A.; Fernández-Escamilla, V. V.; Escalante-García, Z. Y.; Macías-Rodríguez, M. E.; Estrada-Girón, Y. Food Science and Biotechnology 2021, 30, 901-910.
15. Swarna, S.; Govindarajan, V. U.; Anbalagan, A.; Christopher, D.; Muthuraman, M. S. Biomass Conversion and Biorefinery 2024, 1-12.
16. Filimon, A.; Dobos, A. M.; Onofrei, M. D.; Serbezeanu, D. Polymers 2025, 17, 1016.
17. Sunarwidhi, A. L.; Hernawan, A.; Frediansyah, A.; Widyastuti, S.; Martyasari, N. W. R.; Abidin, A. S.; Padmi, H.; Handayani, E.; Utami, N. W. P.; Maulana, F. A. Molecules 2022, 27, 7509.
18. Rahman Khan, M. M.; Rumon, M. M. H.; Islam, M. Processes 2024, 12.
19. Pathak, V.; Lad, P.; Thakkar, A. B.; Thakor, P.; Deshpande, M.; Pandya, S. Results in Surfaces and Interfaces 2023, 11, 100111.
20. Truzzi, E.; Marchetti, L.; Bertelli, D.; Benvenuti, S. Phytochemical analysis 2021, 32, 907-920.
21. Jaison, J. P.; Balasubramanian, B.; Gangwar, J.; Pappuswamy, M.; Meyyazhagan, A.; Kamyab, H.; Paari, K. A.; Liu, W.-C.; Taheri, M. M.; Joseph, K. S. Bioprocess and Biosystems Engineering 2024, 47, 1605-1618.
22. Ullah, H.; Usman, F.; Rasheed, M. A.; Khan, A. A.; Ahmad, R.; Lee, S. Y.; Heo, J.; Ali, G.; Khan, M.; Cho, S. O. ACS Applied Nano Materials 2022, 5, 9096-9111.
23. Safari, P.; Rahimabadi, E. Z.; Vaezi, M. R.; Behnamghader, A.; Tahergorabi, R. Scientific Reports 2025, 15, 1-17.
24. Mobarak, M. B.; Hossain, M. S.; Chowdhury, F.; Ahmed, S. Arabian Journal of Chemistry 2022, 15, 104117.
25. Mani, V. M.; Kalaivani, S.; Sabarathinam, S.; Vasuki, M.; Soundari, A. J. P. G.; Das, M. A.; Elfasakhany, A.; Pugazhendhi, A. Environmental Research 2021, 201, 111502.
26. Rasheed, R.; Uzair, B.; Raza, A.; Binsuwaidan, R.; Alshammari, N. Frontiers in Cellular and Infection Microbiology 2024, 14, 1301351.
27. Trinh, P. T. N.; Truc, N. C.; Danh, T. T.; Trang, N. T. T.; Le Hang, D. T.; Vi, L. N. T.; Hung, Q. T.; Dung, L. T. Journal of Ethnopharmacology 2024, 334, 118519.
28. Hasan, E. A.; El-Hashash, M. A.; Zahran, M. K.; El-Rafie, H. M. Journal of Drug Delivery Science and Technology 2022, 67, 103005.
29. Maji, P.; Pal, D. Applied Physics A 2024, 130, 637.
30. Nandiyanto, A. B. D.; Ragadhita, R.; Fiandini, M. Indonesian Journal of Science and Technology 2023, 8, 113-126.
31. Pasieczna-Patkowska, S.; Cichy, M.; Flieger, J. Molecules 2025, 30, 684.
32. Ali, K.; Sajid, M.; Bakar, S. A.; Younus, A.; Ali, H.; Rashid, M. Z. Hybrid Advances 2024, 6, 100250.
33. Paul, C. A.; Kumar, E. R.; Suryakanth, J.; Abd El-Rehim, A. Ceramics International 2023, 49, 31193-31209.
34. Le, T. D. H.; Tuan, H. N. A.; Nguyen, V. T.; Le, A. T. Journal of Sol-Gel Science and Technology 2023, 107, 441-451.
35. Harish, V.; Tewari, D.; Gaur, M.; Yadav, A. B.; Swaroop, S.; Bechelany, M.; Barhoum, A. Nanomaterials 2022, 12, 457.
36. Ramezani, M.; Ripin, Z. M. Journal of Composites Science 2023, 7, 199.
37. Alhalili, Z. Arabian Journal of Chemistry 2022, 15, 103739.
38. Pochapski, D. J.; Carvalho dos Santos, C.; Leite, G. W.; Pulcinelli, S. H.; Santilli, C. V. Langmuir 2021, 37, 13379-13389.
39. Yu, C.; Dou, X.; Meng, L.; Feng, X.; Gao, C.; Chen, F.; Tang, X. International Journal of Biological Macromolecules 2023, 253, 127618.
40. Asif, H. M.; Zafar, F.; Ahmad, K.; Iqbal, A.; Shaheen, G.; Ansari, K. A.; Rana, S.; Zahid, R.; Ghaffar, S. Scientific Reports 2023, 13, 10274.